Supplementary Information (SI) for Materials Advances.
This journal is © The Royal Society of Chemistry 2026

Supplementary Information

1. The glass transition width and its dependence on fragility, nonexponentiality and nonlinearity

This paper presents a comprehensive and critical analysis of the glass transition width ($1/T_g$ -$1/T_g$') or or ($\Delta T_g/T_g$') observed in calculated Differential Scanning Calorimetry (DSC) heating and cooling scans. The study uses the Tool-Narayanaswamy-Moynihan model (TNM) for 24 diverse materials, encompassing inorganic glasses, organic polymers and molecular glassy systems (shown in Fig.S1 – Fig.S24). The analysis reveals that the width of the glass transition cooling scan does not depend on scanning rate and is inversely proportional to the activation energy, or fragility m, and the sum of the non-exponentiality β and nonlinearity x parameters: $[(h^*/R)\cdot(\beta+x)]^{-1}$ or $[m\cdot(\beta+x)]^{-1}$. The proportionality constant depends on the specific method used to determine T_g and T_g' values. Fig.S1 – Fig.S24 illustrate how these values are determined from the calculated DSC cooling curves (-10 K/min) for all material types listed in Table 1 (green lines). The determination of the limiting fictive temperature is illustrated using the subsequent heating curves at a rate of +10 K/min.

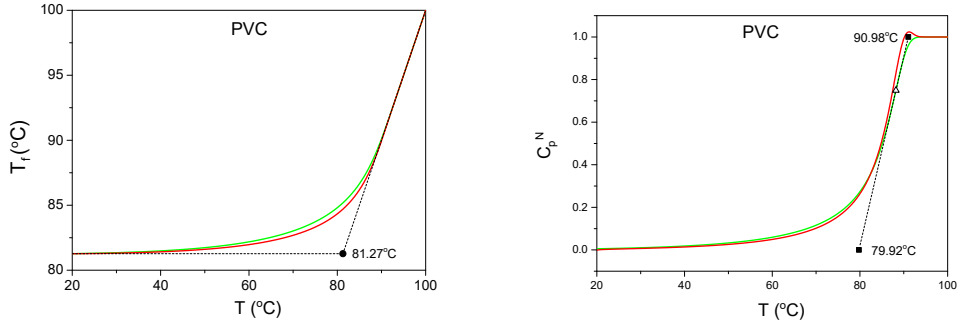

Fig.S1 The fictive temperature T_f and normalized heat capacity C_p^N calculated for poly(vinyl chloride).[1] The TNM parameters are listed in Table 1 and the temperature program is T_{ini}= 100°C, q_c = -10 K/min (green line), q_h = +10 K/min (red line). Open triangle indicates inflection point on cooling curve. Full squares correspond to extrapolated inflectional tangent intersection with dT_f/dT = 0 and dT_f/dT = 1 defining T_g and T_g', respectively. Full circle indicates limiting fictive temperature.

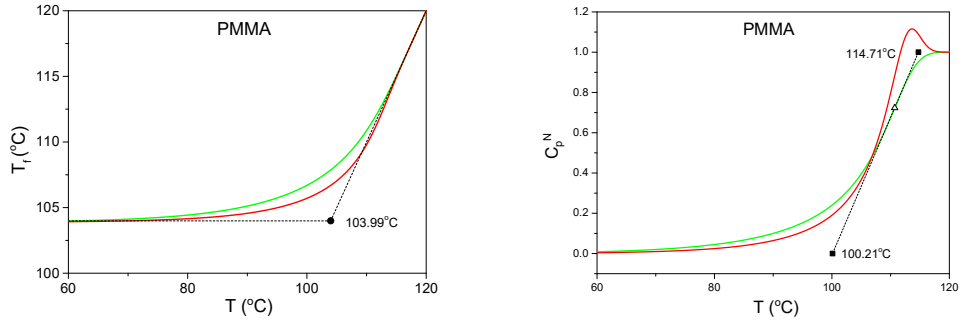

Fig.S2 The fictive temperature T_f and normalized heat capacity C_p^N calculated for poly(methyl methacrylate).[1] The TNM parameters are listed in Table 1 and the temperature program is T_{ini}= 120°C, q_c = -10 K/min (green line), q_h = +10 K/min (red line). Open triangle indicates inflection point on cooling curve. Full squares correspond to extrapolated inflectional tangent intersection with dT_f/dT = 0 and dT_f/dT = 1 defining T_g and T_g', respectively. Full circle indicates limiting fictive temperature.

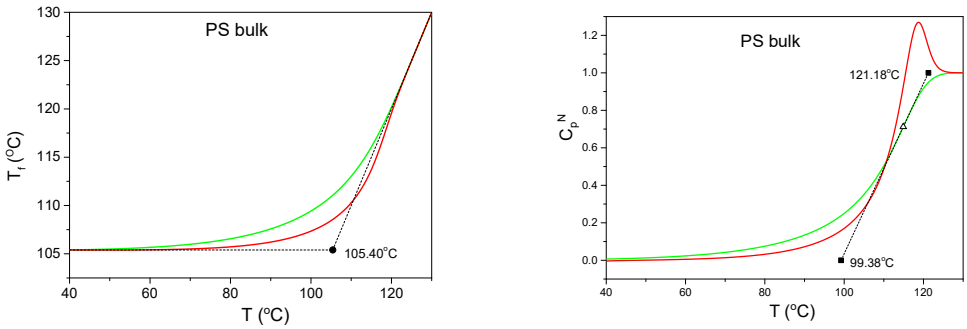

Fig.S3 The fictive temperature T_f and normalized heat capacity C_p^N calculated for bulk polystyrene.[2] The TNM parameters are listed in Table 1, and the temperature program is T_{ini}= 130°C, q_c = -10 K/min (green line), q_h = +10 K/min (red line). Open triangle indicates inflection points on cooling curve. Full squares correspond to extrapolated inflectional tangent intersection with dT_f/dT = 0 and dT_f/dT = 1 defining T_g and T_g', respectively. Full circle indicates limiting fictive temperature.

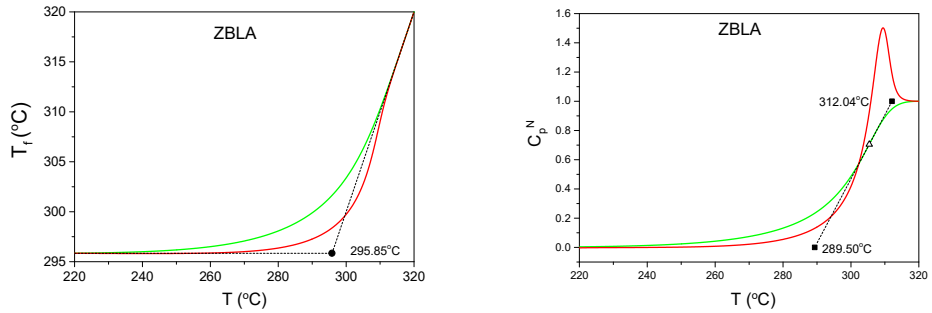

Fig.S4 The fictive temperature T_f and normalized heat capacity C_p^N calculated for ZBLAN fluoride glass ($58ZrF_4$-$33BaF_2$-$5LaF_3$-$4AlF_3$).[3] The TNM parameters are listed in Table 1, and the temperature program is T_{ini}= 320°C, q_c = -10 K/min (green line), q_h = +10 K/min (red line). Open triangle indicates inflection point on cooling curve. Full squares correspond to extrapolated inflectional tangent intersection with dT_f/dT = 0 and dT_f/dT = 1 defining T_g and T_g', respectively. Full circle indicates limiting fictive temperature.

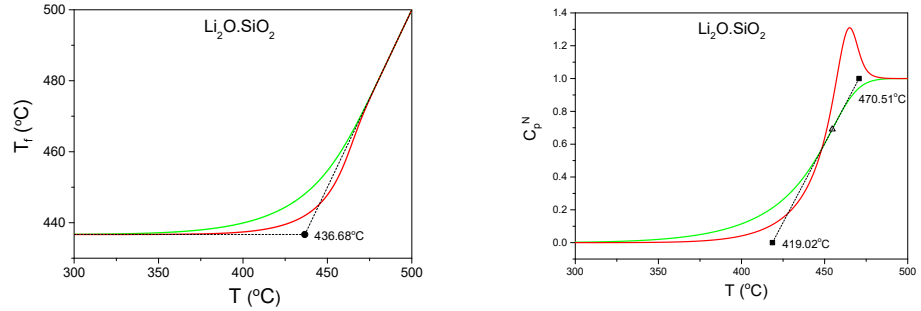

Fig.S5 The fictive temperature T_f and normalized heat capacity C_p^N calculated for $Li_2O.SiO_2$ glass.[4] The TNM parameters are listed in Table 1, and the temperature program is T_{ini}= 500°C, q_c = -10 K/min (green line), q_h = +10 K/min (red line). Open triangle indicates inflection point on cooling curve. Full squares correspond to extrapolated inflectional tangent intersection with dT_f/dT = 0 and dT_f/dT = 1 defining T_g and T_g', respectively. Full circle indicates limiting fictive temperature.

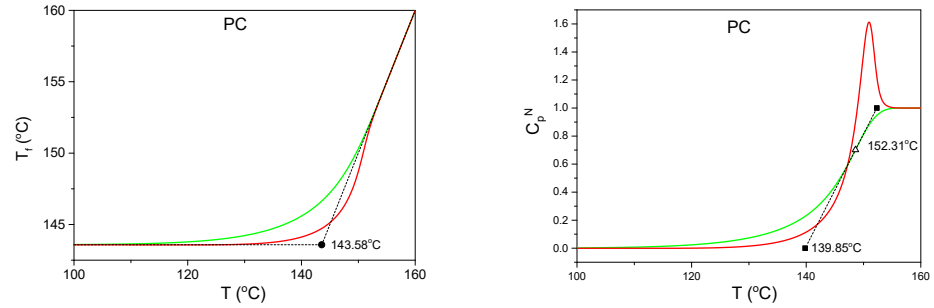

Fig.S6 The fictive temperature T_f and normalized heat capacity C_p^N calculated for polycarbonate.[5] The TNM parameters are listed in Table 1, and the temperature program is T_{ini}= 160°C, q_c = -10 K/min (green line), q_h = +10 K/min (red line). Open triangle indicates inflection point on cooling curve. Full squares correspond to extrapolated inflectional tangent intersection with dT_f/dT = 0 and dT_f/dT = 1 defining T_g and T_g', respectively. Full circle indicates limiting fictive temperature.

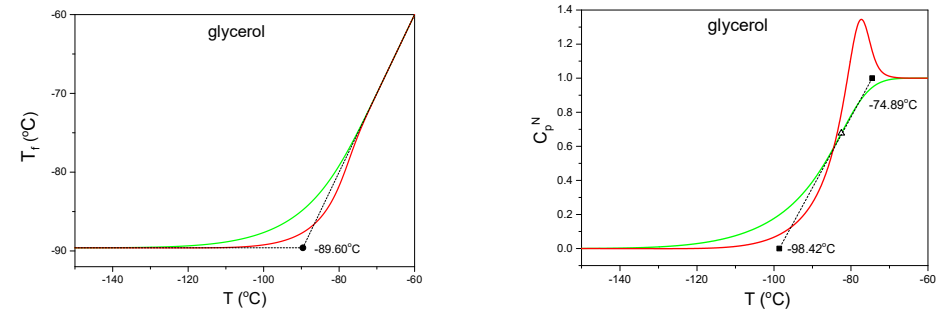

Fig.S7 The fictive temperature T_f and normalized heat capacity C_p^N calculated for glycerol.[6] The TNM parameters are listed in Table 1, and the temperature program is T_{ini}= -60°C, q_c = -10 K/min (green line), q_h = +10 K/min (red line). Open triangle indicates inflection point on cooling curve. Full squares correspond to extrapolated inflectional tangent intersection with dT_f/dT = 0 and dT_f/dT = 1 defining T_g and T_g', respectively. Full circle indicates limiting fictive temperature.

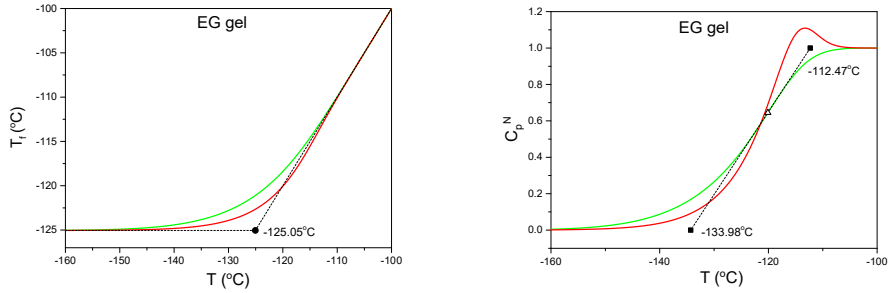

Fig.S8 The fictive temperature T_f and normalized heat capacity C_p^N calculated for ethylene glycol gel (22 mol.% in H_2O).[3] The TNM parameters are listed in Table 1, and the temperature program is T_{ini}= -100°C, q_c = -10 K/min (green line), q_h = +10 K/min (red line). Open triangle indicates inflection point on cooling curve. Full squares correspond to extrapolated inflectional tangent intersection with dT_f/dT = 0 and dT_f/dT = 1 defining T_g and T_g', respectively. Full circle indicates limiting fictive temperature.

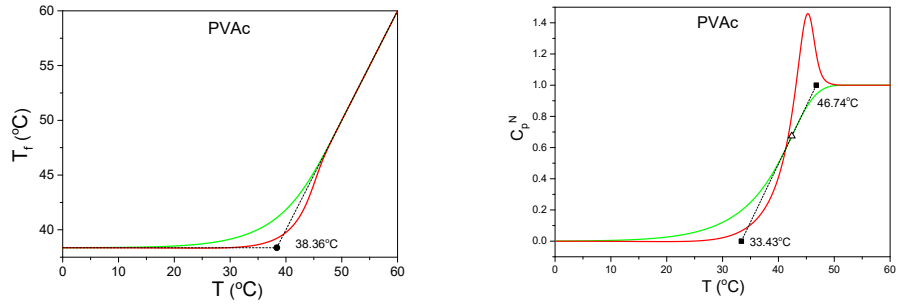

Fig.S9 The fictive temperature T_f and normalized heat capacity C_p^N calculated for poly(vinyl acetate).[7] The TNM parameters are listed in Table 1, and the temperature program is T_{ini}= 60°C, q_c = -10 K/min (green line), q_h = +10 K/min (red line). Open triangle indicates inflection point on cooling curve. Full squares correspond to extrapolated inflectional tangent intersection with dT_f/dT = 0 and dT_f/dT = 1 defining T_g and T_g', respectively. Full circle indicates limiting fictive temperature.

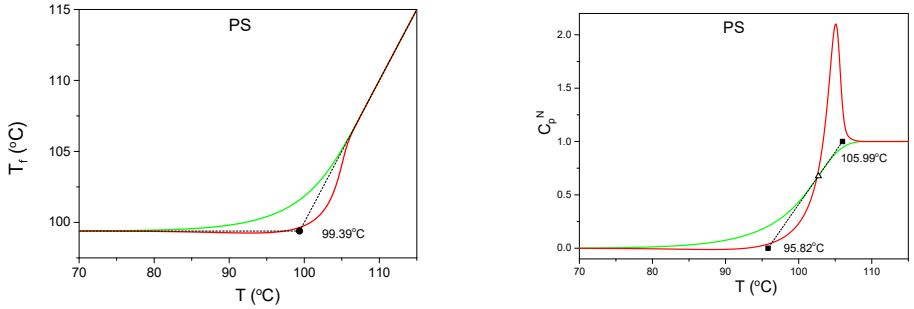

Fig.S10 The fictive temperature T_f and normalized heat capacity C_p^N calculated for polystyrene.[8] The TNM parameters are listed in Table 1, and the temperature program is T_{ini}= 115°C, q_c = -10 K/min (green line), q_h = +10 K/min (red line). Open triangle indicates inflection point on cooling curve. Full squares correspond to extrapolated inflectional tangent intersection with dT_f/dT = 0 and dT_f/dT = 1 defining T_g and T_g', respectively. Full circle indicates limiting fictive temperature.

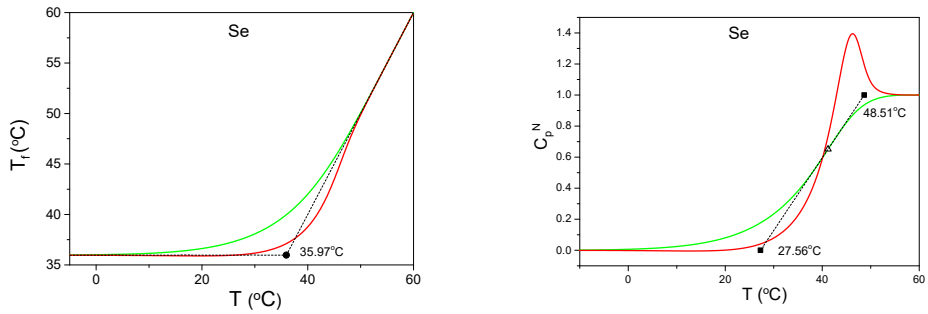

Fig.S11 The fictive temperature T_f and normalized heat capacity C_p^N calculated for glassy selenium.[9] The TNM parameters are listed in Table 1, and the temperature program is T_{ini}= 60°C, q_c = -10 K/min (green line), q_h = +10 K/min (red line). Open triangle indicates inflection point on cooling curve. Full squares correspond to extrapolated inflectional tangent intersection with dT_f/dT = 0 and dT_f/dT = 1 defining T_g and T_g', respectively. Full circle indicates limiting fictive temperature.

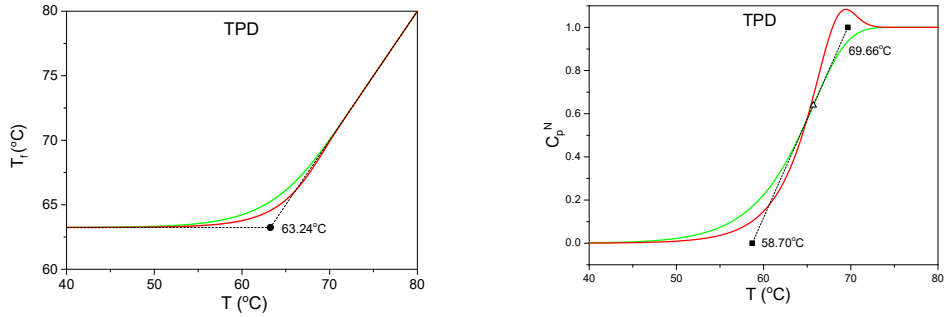

Fig.S12 The fictive temperature T_f and normalized heat capacity C_p^N calculated for bulk TPD.[10] The TNM parameters are listed in Table 1, and the temperature program is T_{ini}= 80°C, q_c = -10 K/min (green line), q_h = +10 K/min (red line). Open triangle indicates inflection point on cooling curve. Full squares correspond to extrapolated inflectional tangent intersection with dT_f/dT = 0 and dT_f/dT = 1 defining T_g and T_g', respectively. Full circle indicates limiting fictive temperature.

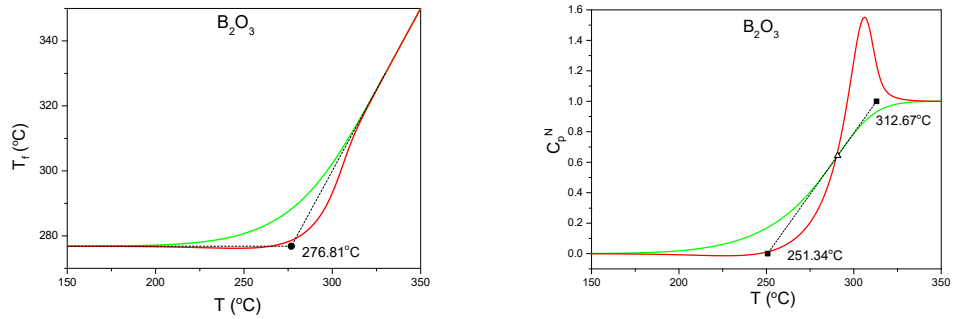

Fig.S13 The fictive temperature T_f and normalized heat capacity C_p^N calculated for B_2O_3.[11] The TNM parameters are listed in Table 1, and the temperature program is T_{ini}= 350°C, q_c = -10 K/min (green line), q_h = +10 K/min (red line). Open triangle indicates inflection point on cooling curve. Full squares correspond to extrapolated inflectional tangent intersection with dT_f/dT = 0 and dT_f/dT = 1 defining T_g and T_g', respectively. Full circle indicates limiting fictive temperature.

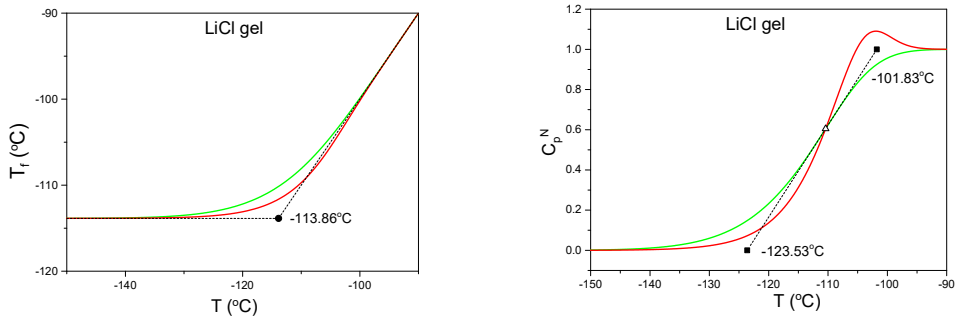

Fig.S14 The fictive temperature T_f and normalized heat capacity C_p^N calculated for LiCl gel.[12] The TNM parameters are listed in Table 1, and the temperature program is T_{ini}= -90°C, q_c = -10 K/min (green line), q_h = +10 K/min (red line). Open triangle indicates inflection point on cooling curve. Full squares correspond to extrapolated inflectional tangent intersection with dT_f/dT = 0 and dT_f/dT = 1 defining T_g and T_g', respectively. Full circle indicates limiting fictive temperature.

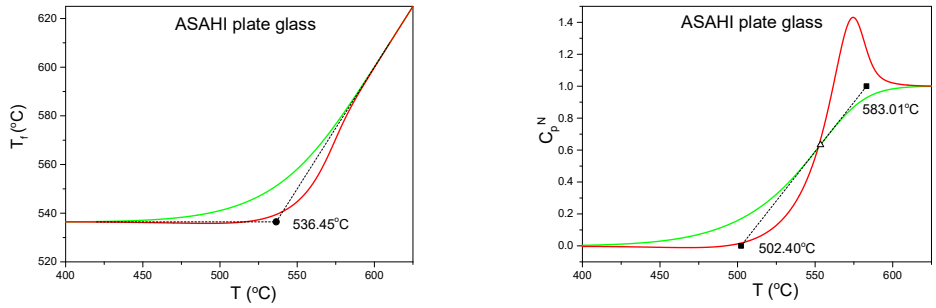

Fig.S15 The fictive temperature T_f and normalized heat capacity C_p^N calculated for ASAHI plate glass.[13] The TNM parameters are listed in Table 1, and the temperature program is T_{ini}= -625°C, q_c = -10 K/min (green line), q_h = +10 K/min (red line). Open triangle indicates inflection point on cooling curve. Full squares correspond to extrapolated inflectional tangent intersection with dT_f/dT = 0 and dT_f/dT = 1 defining T_g and T_g', respectively. Full circle indicates limiting fictive temperature.

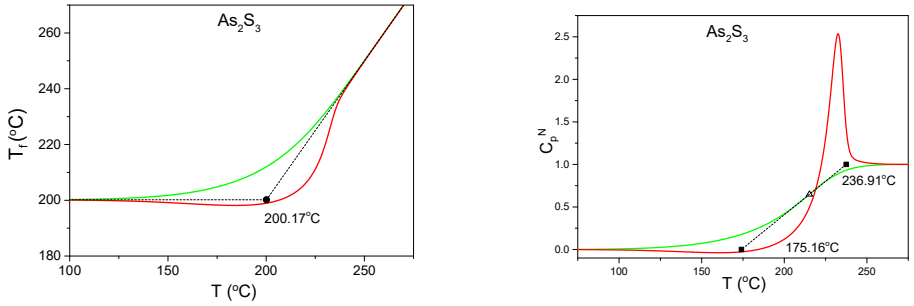

Fig.S16 The fictive temperature T_f and normalized heat capacity C_p^N calculated for As_2S_3 glass.[14] The TNM parameters are listed in Table 1, and the temperature program is T_{ini}= 275°C, q_c = -10 K/min (green line), q_h = +10 K/min (red line). Open triangle indicates inflection point on cooling curve. Full squares correspond to extrapolated inflectional tangent intersection with dT_f/dT = 0 and dT_f/dT = 1 defining T_g and T_g', respectively. Full circle indicates limiting fictive temperature.

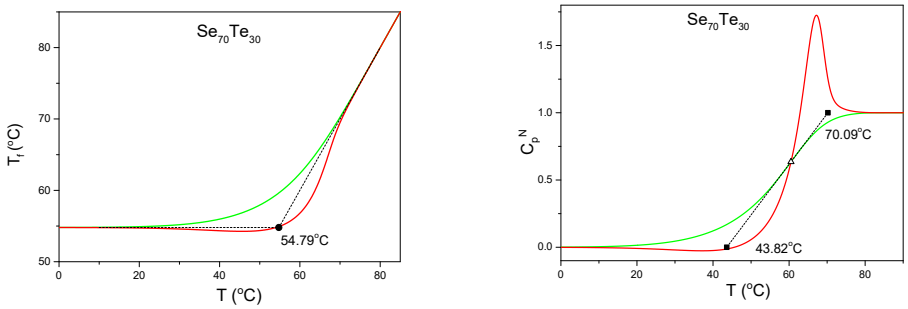

Fig.S17 The fictive temperature T_f and normalized heat capacity C_p^N calculated for $Se_{70}Te_{30}$ glass.[15] The TNM parameters are listed in Table 1, and the temperature program is T_{ini}= 85°C, q_c = -10 K/min (green line), q_h = +10 K/min (red line). Open triangle indicates inflection point on cooling curve. Full squares correspond to extrapolated inflectional tangent intersection with dT_f/dT = 0 and dT_f/dT = 1 defining T_g and T_g', respectively. Full circle indicates limiting fictive temperature.

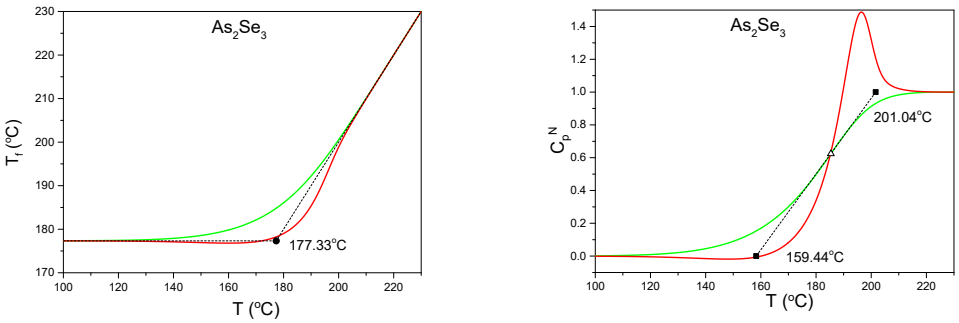

Fig.S18 The fictive temperature T_f and normalized heat capacity C_p^N calculated forAs_2Se_3 glass.[16] The TNM parameters are listed in Table 1, and the temperature program is T_{ini}= 230°C, q_c = -10 K/min (green line), q_h = +10 K/min (red line). Open triangle indicates inflection point on cooling curve. Full squares correspond to extrapolated inflectional tangent intersection with dT_f/dT = 0 and dT_f/dT = 1 defining T_g and T_g', respectively. Full circle indicates limiting fictive temperature.

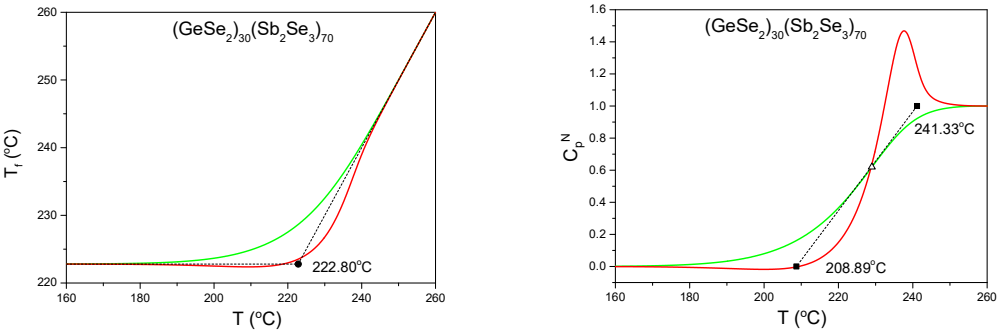

Fig.S19 The fictive temperature T_f and normalized heat capacity C_p^N calculated for $(GeSe_2)_{30}$ $(Sb_2Se_3)_{70}$ glass.[17] The TNM parameters are listed in Table 1, and the temperature program is T_{ini}= 260°C, q_c = -10 K/min (green line), q_h = +10 K/min (red line). Open triangle indicates inflection point on cooling curve. Full squares correspond to extrapolated inflectional tangent intersection with dT_f/dT = 0 and dT_f/dT = 1 defining T_g and T_g', respectively. Full circle indicates limiting fictive temperature.

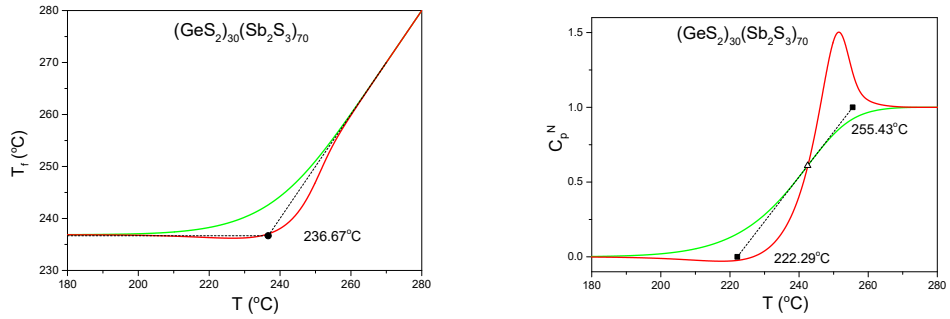

Fig.S20 The fictive temperature T_f and normalized heat capacity C_p^N calculated for $(GeS_2)_{30}(Sb_2S_3)_{70}$ glass.[18] The TNM parameters are listed in Table 1, and the temperature program is T_{ini}= 280°C, q_c = -10 K/min (green line), q_h = +10 K/min (red line). Open triangle indicates inflection point on cooling curve. Full squares correspond to extrapolated inflectional tangent intersection with dT_f/dT = 0 and dT_f/dT = 1 defining T_g and T_g', respectively. Full circle indicates limiting fictive temperature.

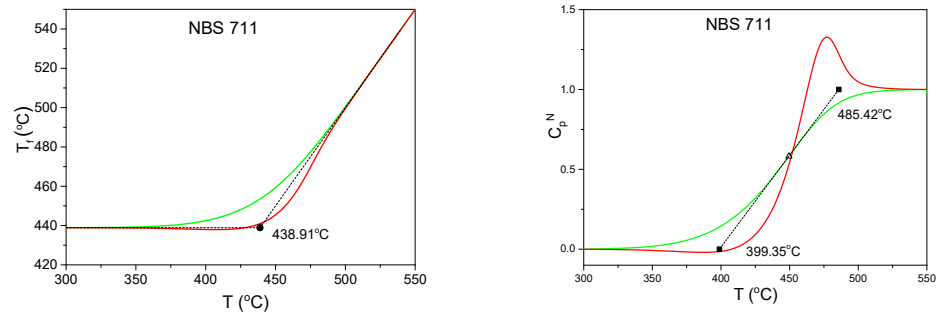

Fig.S21 The fictive temperature T_f and normalized heat capacity C_p^N calculated for NBS711 glass.[19] The TNM parameters are listed in Table 1, and the temperature program is T_{ini}= 550°C, q_c = -10 K/min (green line), q_h = +10 K/min (red line). Open triangle indicates inflection point on cooling curve. Full squares correspond to extrapolated inflectional tangent intersection with dT_f/dT = 0 and dT_f/dT = 1 defining T_g and T_g', respectively. Full circle indicates limiting fictive temperature.

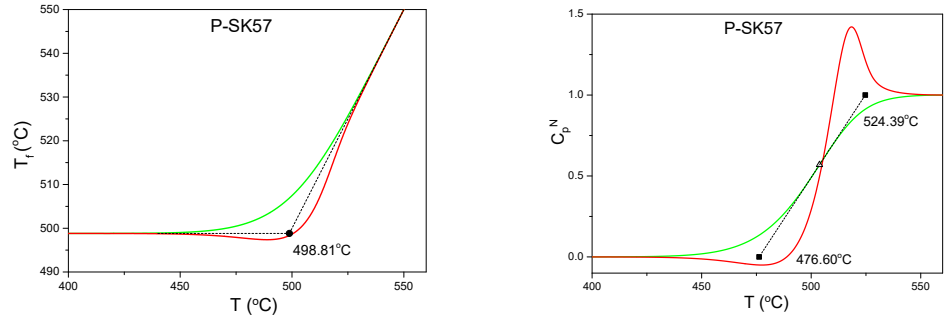

Fig.S22 The fictive temperature T_f and normalized heat capacity C_p^N calculated for P-SK57 glass.[20] The TNM parameters are listed in Table 1, and the temperature program is T_{ini}= 560°C, q_c = -10 K/min (green line), q_h = +10 K/min (red line). Open triangle indicates inflection point on cooling curve. Full squares correspond to extrapolated inflectional tangent intersection with dT_f/dT = 0 and dT_f/dT = 1 defining T_g and T_g', respectively. Full circle indicates limiting fictive temperature.

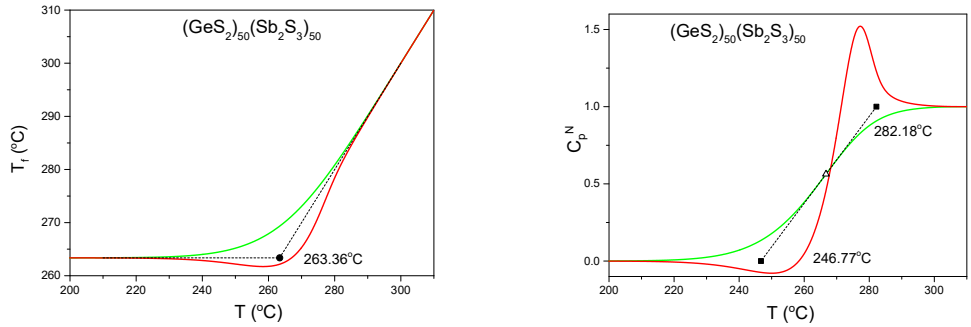

Fig.S23 The fictive temperature T_f and normalized heat capacity C_p^N calculated for $(GeS_2)_{50}(Sb_2S_3)_{50}$ glass.[21] The TNM parameters are listed in Table 1, and the temperature program is T_{ini}= 310°C, q_c = -10 K/min (green line), q_h = +10 K/min (red line). Open triangle indicates inflection point on cooling curve. Full squares correspond to extrapolated inflectional tangent intersection with dT_f/dT = 0 and dT_f/dT = 1 defining T_g and T_g', respectively. Full circle indicates limiting fictive temperature.

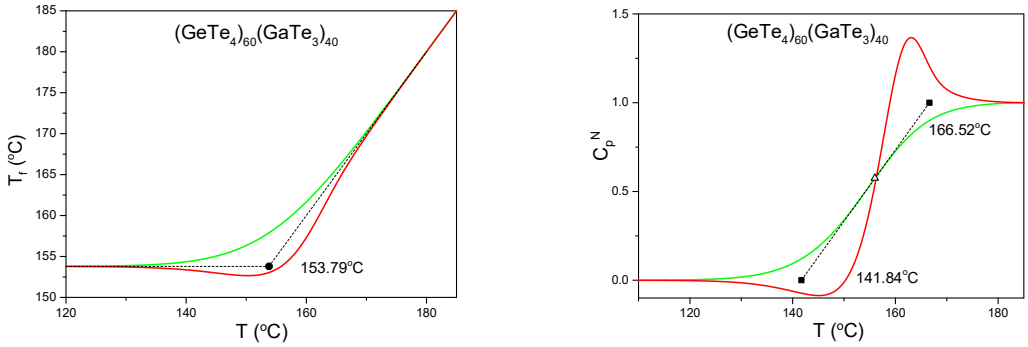

Fig.S24 The fictive temperature T_f and normalized heat capacity C_p^N calculated for $(GeTe_4)_{60}(GaTe_3)_{40}$ glass.[22] The TNM parameters are listed in Table 1, and the temperature program is T_{ini}= 185°C, q_c = -10 K/min (green line), q_h = +10 K/min (red line). Open triangle indicates inflection point on cooling curve. Full squares correspond to extrapolated inflectional tangent intersection with $dT_f/dT = 0$ and $dT_f/dT = 1$ defining T_g and T_g', respectively. Full circle indicates limiting fictive temperature.

2. Covariance and correlation matrices for linear fits shown in Fig.2 – Fig.8

Fig.2b Glass transition width (eq 9) as a function of $[(h^*/R)\cdot\beta]^{-1}$.

Covariance matrix

	Intercept	Slope
Intercept	-	-
Slope	-	0.00399

Correlation matrix

	intercept	slope
Intercept	-	-
Slope	-	1

Fig.2c Reduced glass transition width (eq 10) as a function of $[m\cdot\beta]^{-1}$.

Covariance matrix

	Intercept	Slope
Intercept	-	-
Slope	-	0.00177

Correlation matrix

	intercept	slope
Intercept	-	-
Slope	-	1

Fig.3b Glass transition width (eq 12) as a function of $[(h^*/R)\cdot(\beta+x)]^{-1}$.

Covariance matrix

	Intercept	Slope
Intercept	-	-
Slope	-	0.02927

Correlation matrix

	intercept	slope
Intercept	-	-
Slope	-	1

Fig.3c Reduced glass transition width (eq 13) as a function of $[m\cdot(\beta+x)]^{-1}$.

Covariance matrix

	Intercept	Slope
Intercept	-	-
Slope	-	0.00559

Correlation matrix

	intercept	slope
Intercept	-	-
Slope	-	1

Fig.5a Glass transition width defined by eq (12).

Covariance matrix			**Correlation matrix**	
	Intercept	Slope	intercept	slope
Intercept	-	-	-	-
Slope	-	0.00222	-	1

Fig.5b Reduced glass transition width defined by eq (13).

Covariance matrix			**Correlation matrix**	
	Intercept	Slope	intercept	slope
Intercept	-	-	-	-
Slope	-	0.00096	-	1

Fig.6 Determination of the activation energy (h*/R) and the glass transition width $\Delta(1000/T_g)_c$ using the cooling curves for PVC and As_2S_3 presented in Fig.5.

T_g for As_2S_3

Covariance matrix			**Correlation matrix**	
	Intercept	Slope	intercept	slope
Intercept	0.0148	-0.00063	1	-0.99825
Slope	-0.00063	0.000272	-0.99825	1

T_g' for As_2S_3

Covariance matrix			**Correlation matrix**	
	Intercept	Slope	intercept	slope
Intercept	0.0148	-0.00063	1	-0.99825
Slope	-0.00063	0.000272	-0.99825	1

T_g for PVC

Covariance matrix			**Correlation matrix**	
	Intercept	Slope	intercept	slope
Intercept	5.39206	-1.86204	1	-0.99998
Slope	-1.86204	0.64305	-0.99998	1

T_g' for PVC

Covariance matrix			**Correlation matrix**	
	Intercept	Slope	intercept	slope
Intercept	5.27085	-1.90366	1	-0.99997
Slope	-1.90366	0.68758	-0.99997	1

Fig.7b Evaluation of $\ln|q_1|$ and $\ln|q_2|$ at $1000/T=2.4\ K^{-1}$ based on the cooling curves presented in Fig.7a.

T_g

Covariance matrix

	Intercept	Slope
Intercept	0.01021	-0.0042
Slope	-0.0042	0.00173

Correlation matrix

	intercept	slope
Intercept	1	-0.99896
Slope	-0.99896	1

T_g'

Covariance matrix

	Intercept	Slope
Intercept	0.00178	-0.00075
Slope	-0.00075	0.000317

Correlation matrix

	intercept	slope
Intercept	1	-0.99892
Slope	-0.99892	1

Fig.8a Dependence of the parameter E (calculated by eq 11 for data shown in Table 1) on 1/(β+x).

z = 0.15

Covariance matrix

	Intercept	Slope
Intercept	0.02498	-0.01859
Slope	-0.01859	0.01665

Correlation matrix

	intercept	slope
Intercept	1	-0.91148
Slope	-0.91148	1

z = 0.30

Covariance matrix

	Intercept	Slope
Intercept	0.00742	-0.00552
Slope	-0.00552	0.00495

Correlation matrix

	intercept	slope
Intercept	1	-0.91148
Slope	-0.91148	1

Fig.8b Dependence of the parameter C (calculated by the eq 1) on 1/β

Data in Table 1 (Ref. 1-22)

Covariance matrix

	Intercept	Slope
Intercept	0.1397	-0.06469
Slope	-0.06469	0.03413

Correlation matrix

	intercept	slope
Intercept	1	-0.93683
Slope	-0.93683	1

Chen et al. data (Ref. 23)

Covariance matrix

	Intercept	Slope
Intercept	0.3297	-0.18564
Slope	-0.18564	0.10629

Correlation matrix

	intercept	slope
Intercept	1	-0.9926
Slope	-0.9926	1

References

1 I. M. Hodge, Effects of Annealing and Prior History on Enthalpy Relaxation in Glassy Polymers. 6. Adam-Gibbs Formulation of Nonlinearity, *Macromolecules*, 1987, **20**, 2897-2908.
2 Y. Guo, C. Zhang, C. Lai, R. D. Priestley, M. D'Acunzi, G. Fytas, Structural Relaxation of Polymer Nanospheres under Soft and Hard Confinement: Isobaric versus Isochoric Conditions, *ACS Nano*, 2011, **5**, 5365-73.
3 I. M. Hodge, Enthalpy relaxation and recovery in amorphous materials, *J. Non-Cryst. Solids*, 1994, **169**, 211-66.
4 Y. Han, A. D'Amore, N. Nicolais, Analysis of Structural Relaxtion in a $Li_2O.2SiO_2$ Glass using Rate Heating Approach, *J. Mater. Sci.*, 1999, **34**, 1899-1904.
5 I. M. Hodge, Effects of Annealing and Prior History on Enthalpy Relaxation in Glassy Polymers. 4. Comparison of Five Polymers, *Macromolecules*, 1983, **16**, 898-902.
6 S. L. Simon, G. B. McKenna, Interpretation of the dynamic heat capacity observed in glass-forming liquids, *J. Chem. Phys.*, 1997, **107**, 8678-85.
7 H. Sasabe, C. T. Moynihan, Structural Relaxation in Poly(vinyl Acetate), *J. Polym. Sci.*, 1978, **16**, 1447-57.
8 Y. P. Koh, S. L. Simon, Enthalpy Recovery of Polystyrene: Does a Long-Term Aging Plateau Exist? *Macromolecules*, 2013, **46**, 5815-21.
9 J. Málek, R. Svoboda, P. Pustková, P. Čičmanec, Volume and enthalpy relaxation of a-Se in the glass transition region, *J. Non-Cryst. Solids.*, 2009, **355**, 264-272.
10 J. Málek, R. Svoboda, Remarkable difference in structural relaxation dynamics of conventionally prepared bulk glass and vapor-deposited thin films, *J. Chem. Phys.*, 2024, **161**, 074507.
11 M. A. DeBolt, A. J. Easteal, P. B. Macedo, C. T. Moynihan, Analysis of Structural Relaxation in Glass Using Rate Heating Data, *J. Am. Ceram. Soc.,* 1976, **59**, 16-21.
12 I. M. Hodge, Enthalpy relaxation and recovery in amorphous materials, *J. Non-Cryst. Solids*, 1994, **169**, 211-66.
13 G. W. Scherer, Volume relaxation far from equilibrium, *J. Am. Ceram. Soc.*, 1986, **69**, 374-81.
14 J. Málek, Dilatometric study of structural relaxation in arsenic sulfide glass, *Thermochim. Acta*, 1998, **311**, 183-98.
15 R. Svoboda, P. Honcová, J. Málek J. Enthalpic structural relaxation in Se-Te glassy system. *J. Non-Cryst. Solids*, 2011, **357**, 2163-9.
16 A. J. Easteal, J. A. Wilder, R. K. Mohr, C. T. Moynihan, Heat Capacity and Structural Relaxation of Enthalpy in As_2Se_3 Glass, *J. Am. Ceram. Soc.*, 1977, **60**, 134-8.
17 R. Svoboda, J. Málek, M. Liška,Correlation between the structure and structural relaxation data for $(GeSe_2)_y(Sb_2Se_3)_{1-y}$ glasses, *J. Non-Cryst. Solids*. 2019, **505**, 162-9.
18 R. Svoboda, J. Málek, M. Liška,Correlation between the structure and relaxation dynamics of $(GeS_2)_y(Sb_2S_3)_{1-y}$ glassy matrices, *J. Non-Cryst. Solids*, 2018, **479**, 113-9.
19 S. N. Crichton, C. T. Moynihan, Structural relaxation of lead silicate glass, *J. Non-Cryst. Solids*, 1988, **102**, 222-7.
20 S. Gaylord, B. Ananthasayanam, B. Tincher, L. Petit, C. Cox, U. Fotteringham, P. Joseph, K. Richardson, Thermal and Structural Property Characterization of Commercially Moldable Glasses, *J. Am. Ceram. Soc*, 2010, **93**, 2207-14.
21 R. Svoboda, M. Fraenkel, B. Frumarová, T. Wágner, J. Málek, Thermokinetic behaviour of Ag-doped $(GeS_2)_{50}(Sb_2S_3)_{50}$ glasses, *J. Non-Cryst. Solids*, 2016, **449**, 12-9.
22 R. Svoboda, M. Setnička, Z. Zmrhalová, D. Brandová, J. Málek, Structural interpretation of the enthalpy relaxation kinetics of $(GeTe_4)_y(GaTe_3)_{1-y}$ far-infrared glasses, *J. Non-Cryst. Solids*, 2016, **447**, 110-6.
23 Z. Chen, L. Zhao, W. Tu, Z. Li, Y. Gao, L. Wang, Dependence of calorimetric glass transition profiles on relaxation dynamics in non-polymeric glass-formers, *J. Non-Cryst. Solids*, 2016, **433**, 20-27.